



# Prediction of the activity concentrations of $^{232}\text{Th}$ , $^{238}\text{U}$ and $^{40}\text{K}$ in geological materials using radial basis function neural network

Selin Erzin<sup>1</sup> · Günseli Yaprak<sup>2</sup>

Received: 6 February 2022 / Accepted: 8 July 2022 / Published online: 5 August 2022  
© Akadémiai Kiadó, Budapest, Hungary 2022

## Abstract

In this paper, three individual models and one generalized radial basis function neural network (RBFNN) model were developed for the prediction of the activity concentrations of primordial radionuclides, namely,  $^{232}\text{Th}$ ,  $^{238}\text{U}$  and  $^{40}\text{K}$ . To achieve this, gamma spectrometry measurements of 126 different geological materials were used in the development of the RBFNN models. The results indicated that individual and generalized RBFNN models are quite efficient in predicting the activity concentrations of  $^{232}\text{Th}$ ,  $^{238}\text{U}$  and  $^{40}\text{K}$  of geological materials.

**Keywords** Gamma spectrometry · NaI(Tl) detector · Neural networks · Radial basis function

## Introduction

Human population have continuously been exposed to natural radiation, which is partially because of the activity concentration of primordial radionuclides, namely,  $^{232}\text{Th}$  series,  $^{238}\text{U}$  ( $^{226}\text{Ra}$ ) series and  $^{40}\text{K}$  [1]. These primordial radionuclides exist in the earth's crust, building materials, air, water, foods and in the human body itself [1]. These exposures may change with the local geology of each region in the world. The knowledge of the distribution of primordial radionuclides plays a significant role for people seeking to avoid long-term exposure. The activity concentration of primordial radionuclides is determined by gamma-ray spectrometry methods using low resolution NaI(Tl) and high resolution HPGe or equivalent detectors [2]. NaI(Tl) detectors in spite of their low resolution are the most common and widely used detectors for making qualitative and quantitative analysis of natural and artificial radionuclides in various samples [3, 4]. There have been many radiological surveys to determine the background radionuclide levels in soil samples and their radiological hazards [5–13].

In mathematical modelling, a special type of artificial neural network (ANN), namely, radial basis function neural network (RBFNN) uses radial basis functions as activation function [14]. RBFNN is specifically used for prediction and classification purposes [15]. RBFNN typically has three layers with the first one being input layer, the second one being hidden layer with a non-linear radial basis function as activation function and the last one being linear output layer [16, 17]. Similar to neural networks and fuzzy inference systems, RBFNN with a simple structure, including one hidden layer, can approximate any function [18]. Thus, RBFNN are called as universal approximators [19]. The design and training stages of RBFNN are much faster and easier than multi-layer perceptron (MLP) networks (i.e., traditional ANNs). From the point of generalization, RBFNN are capable of responding perfectly for patterns which are not used for training [18]. RBFNN have strong tolerance to input noise which enhances the stability of the designed systems [18]. Thus, it is reasonable to consider RBFNN as a competitive method of nonlinear controller design [18]. Because of their universal approximation, more compact topology, and faster learning speed than MLP networks, RBFNN have attracted much attention and they have been widely applied in many science and engineering fields [20].

With this in mind, RBFNN models were developed for predicting the activity concentrations of primordial radionuclides  $^{232}\text{Th}$ ,  $^{238}\text{U}$  and  $^{40}\text{K}$ . To achieve this, gamma spectrometry measurements of 126 different geological materials were made using a NaI(Tl) detector [21]. The RBFNN

✉ Selin Erzin  
selin.erzin@deu.edu.tr

<sup>1</sup> Department of Physics, Faculty of Science, Dokuz Eylül University, 35390 Izmir, Turkey

<sup>2</sup> Institute of Nuclear Sciences, Ege University, 35100 Izmir, Turkey

models' results were compared with the results of gamma spectrometry measurements for evaluating the performance of RBFNN models. In addition, the RBFNN models' performance was also checked by computing four different performance parameters.

## Radial basis function neural networks

RBFNNs, developed by Broomhead and Lowe [22], were inspired by the impulse response behaviors seen in biological nerve cells and entered the ANN's history by solving the filtering problem [22]. It is feasible to envision the training of RBFNN models as a curve fitting approach in multidimensional space [23]. Thus, the training performance of the RBFNN model is finding the best surface for the data in the output vector space and hence it turns into an interpolation problem. In RBFNN models, similar to the architecture of ANN, there are three layers: input layer, hidden layer and output layer (Fig. 1). The input layer is made up of source nodes that connect the network to its environment. However, unlike classical ANN structures, radial based activation functions are used in the transition from input layer to hidden layer and a nonlinear cluster analysis is used. The structure between the hidden layer and the output layer is similar to that of other ANN types, with the main training taking place here.

In RBFNN models, the output ( $y$ ) produced by the network is calculated with the help of Eq. 1.

$$y_i = \sum_{k=1}^N w_{ik} \phi_k(x, c_k) = \sum_{k=1}^N w_{ik} \phi_k(\|x - c_k\|_2), \quad i = 1, 2, 3, \dots, m, \quad (1)$$

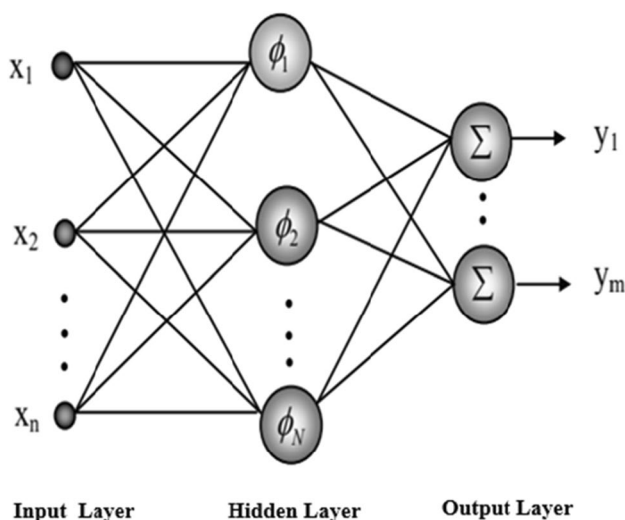


Fig. 1 The structure of RBFNN [15]

where  $x \in R^{n \times 1}$  is network's input vector;  $\phi_k(\cdot) \in R^+$  is the radial based activation function;  $c_k \in R^{n \times 1}$  are the radial-based centers selected from a subset of the input vector space;  $\|\cdot\|_2$  is the Euclidean norm, a measure of how far the vector is from the center;  $w_{ik}$  are output layer's weights;  $N$  is cells' number in the hidden layer [24, 25].

Important elements in RBFNN models are centers of cells, the output layer's weights and the activation function's structure used. On RBFNN models, many types of functions can be used as activation functions, examples of which are Linear, Cubic, Gaussian, Multi-quadratic, Inverse Multi-quadratic functions. The Gauss function is preferred in this study because it is factorizable. Mathematical structure of the Gauss function is shown in Eq. (2).

$$\phi_k(x) = \exp(-\|x - c_k\|_2^2 / 2\sigma^2), \quad (2)$$

where  $x$  is the input vector;  $c_k$  is the centers; and  $\sigma$  is the standard deviation and also is called the spread parameter that affects the performance of the RBFNN model significantly.

Training of the RBFNN models is performed by two actions: finding cell centers and optimizing the weights in the output layer [26]. In the literature, different methods are used to find cell centers ( $c_k$ ) and output weights ( $w_{ik}$ ). The most commonly used methods to find cell centers are  $K$ -means and Kohonen clustering methods. The methods used for finding the output weights are Least Mean Squares (LMS) and Moore–Penrose Pseudo–Pseudo-inverse methods [26]. The spread parameter is usually fixed for all cells. In the literature, approximate equivalences exist for the determination of spread parameter in RBFNN models. However, this parameter can also be determined by trial and error [23].

## Experimental measurements

Gamma spectrometry measurements of 126 different geological materials were performed at the Nuclear Science Institute, Ege University, Izmir, Turkey. A Canberra  $76 \times 76$  mm, high sensitivity NaI(Tl) detector connected to a Nucleus PCA-8000 multichannel analyzer and shielded with 75 mm thick lead bricks to reduce the background counting rate was used. In this study, the calibration uranium and thorium standards in radioactive equilibrium were purchased from International Atomic Energy Agency (IAEA). These standards were then prepared with the same geometry as the geological samples. Similarly, the potassium standard was prepared from pure KCl, purchased from Merck. The activity concentrations of  $^{232}\text{Th}$ ,  $^{238}\text{U}$  and  $^{40}\text{K}$  standards were  $2442 \pm 3\%$  Bq  $\text{kg}^{-1}$ ,  $1458 \pm 3\%$  Bq  $\text{kg}^{-1}$  and  $16,210 \pm 3\%$  Bq  $\text{kg}^{-1}$ , respectively.

The experimental procedure of gamma ray spectroscopy using a NaI(Tl) detector for the activity concentrations of  $^{232}\text{Th}$ ,  $^{238}\text{U}$  and  $^{40}\text{K}$  is well described elsewhere [5, 27, 28]. Thus, it will be briefly presented here. The activity concentrations of primordial radionuclides  $^{232}\text{Th}$ ,  $^{238}\text{U}$  and  $^{40}\text{K}$  were based on the solution of the following three linear equations involving sensitivity factors ( $K_1$ ,  $K_2$  and  $K_3$ ) and stripping ratios ( $\alpha$ ,  $\beta$  and  $\gamma$ ) as gamma ray spectrometer calibration parameters.

$$e\text{Th (Bq kg}^{-1}\text{)} = C(^{232}\text{Th})/K_1, \quad (3)$$

$$e\text{U (Bq kg}^{-1}\text{)} = [C(^{238}\text{U}) - aC(^{232}\text{Th})]/K_2, \quad (4)$$

$$K \text{ (Bq kg}^{-1}\text{)} = [C(^{40}\text{K}) - g[C(^{238}\text{U}) - aC(^{232}\text{Th})] - bC(^{232}\text{Th})]/K_3, \quad (5)$$

where  $C(^{232}\text{Th})$ ,  $C(^{238}\text{U})$  and  $C(^{40}\text{K})$  are count rates in thorium, uranium, and potassium channels or energies (the 1760 keV peak of  $^{214}\text{Bi}$ , the 2610 keV peak of  $^{208}\text{Tl}$  and the 1460 keV peak of radioactive potassium), respectively; the term  $e$  shows series equilibrium conditions being accepted;  $aC(^{232}\text{Th})$  and  $bC(^{232}\text{Th})$  are count rates and contribution from thorium in the uranium and the potassium windows;  $gC(^{238}\text{U})$  is the count rate and the contribution from uranium in the potassium window. Without compensation for these count rates, uranium and potassium concentrations cannot be obtained spectrometrically.

The stripping ratios ( $\alpha$ ,  $\beta$  and  $\gamma$ ), and sensitivity factors ( $K_1$ ,  $K_2$  and  $K_3$ ) are influenced by several parameters, such as, counting geometry, detector volume and also the widths of the selected energy windows, etc. [5, 27, 28]. Therefore, stripping ratios and sensitivity factors should be determined for each gamma spectrometric system. The activity concentrations of  $^{232}\text{Th}$ ,  $^{238}\text{U}$  and  $^{40}\text{K}$  standards were utilized for determining the stripping ratios and sensitivity factors of the gamma spectrometric system used in this study. The measurement time for both activity and background measurement were taken as 10,000 s. The background spectra were used for suppressing the contribution of the natural background for the related radionuclides. Accordingly, factors of  $K_1$ ,  $K_2$  and  $K_3$  were determined as  $8.025 \times 10^{-4}$  counts per 10,000 s per Bq  $\text{kg}^{-1}$  of  $^{232}\text{Th}$ ,  $9.43 \times 10^{-4}$  counts per 10,000 s per Bq  $\text{kg}^{-1}$  of  $^{238}\text{U}$ , and  $2.97 \times 10^{-4}$  counts per 10,000 s per Bq  $\text{kg}^{-1}$  of  $^{40}\text{K}$ , respectively. The ratios  $\alpha$ ,  $\beta$  and  $\gamma$  were found as 0.745, 0.853 and 1.29, respectively.

## Radial basis function neural network models

Activity concentrations of  $^{232}\text{Th}$ ,  $^{238}\text{U}$  and  $^{40}\text{K}$  of 126 geological materials of different origin including rock, soil, granite, marble, and fertilizer samples were systematically obtained with one sigma error and determined in relation to dry weight. The descriptive statistics of the activity concentrations of these primordial radionuclides are given in Table 1.

In this paper, three individual radial basis ANN models denoted as RBFNN-1, RBFNN-2 and RBFNN-3 were developed by using the results of the gamma spectrometry measurements of 126 geological materials for the prediction of the activity concentration of  $^{232}\text{Th}$ ,  $^{238}\text{U}$  and  $^{40}\text{K}$ , respec-

tively. In the RBFNN-1 model developed for the prediction of the activity concentration of  $^{232}\text{Th}$ , the input parameter is selected as the count rate in thorium channels denoted as  $C(^{232}\text{Th})$  and the output parameter is selected as the activity concentration of  $^{232}\text{Th}$ . In the RBFNN-2 model developed for the prediction of the activity concentration of  $^{238}\text{U}$ , the input parameter is chosen as the count rate in uranium channels denoted as  $C(^{238}\text{U})$ , and the output parameter is chosen as the activity concentration of  $^{238}\text{U}$ . In the RBFNN-3 model developed for the prediction of the activity concentration of  $^{40}\text{K}$ , the input parameter is taken as the count rate in potassium channels denoted as  $C(^{40}\text{K})$  and the output parameter is taken as the activity concentration of  $^{40}\text{K}$ . The input and output data used in each individual and generalized RBFNN models were scaled to lie between  $-0.9$  and  $0.9$  by using Eq. (6). In Eq. (6),  $x_{\text{norm}}$  is the normalized value,  $x$  is the actual value, and  $x_{\text{max}}$  and  $x_{\text{min}}$  are the maximum and minimum values.

$$x_{\text{norm}} = 1.8 * \left( \frac{x - x_{\text{min}}}{x_{\text{max}} - x_{\text{min}}} \right) - 0.9. \quad (6)$$

The data were then separated into two subsets: a training set and an independent test set. The training set was

**Table 1** The descriptive statistics of the activity concentrations of  $^{232}\text{Th}$ ,  $^{238}\text{U}$  and  $^{40}\text{K}$  of 126 geological materials

	Activity Concentrations (Bq $\text{kg}^{-1}$ )		
	$^{232}\text{Th}$	$^{238}\text{U}$	$^{40}\text{K}$
No. of samples	126	126	126
Minimum	0.00	0.00	0.00
Maximum	181.58	480.74	11,700.45
Mean	44.54	49.40	1032.66
Standard deviation	35.85	68.83	1589.82

used to develop each RBFNN model. The test set was used to assess the performance of each RBFNN model developed. In total (126 data sets), 101 data sets were used for training and 25 data sets were used for testing.

The neural network toolbox of MATLAB7.0 was utilized both for training and testing stages in each RBFNN model. While developing RBFNN models, the Gauss function, which is the most commonly used activation function [29], was preferred as the activation function for individual RBFNN models. The spread parameter that affects the performance of the RBFNN models significantly was determined as 3 by trial and error.

The performance of the overall RBFNN models can be evaluated by several criteria. In this paper, mean absolute error (MAE), root mean square error (RMSE) and variance account for (VAF) represented by Eqs. (7), (8) and (9), respectively, were also computed to check the performance of the developed RBFNN models.

$$\text{MAE} = \frac{1}{N} \sum_{i=1}^N |(y_i - \hat{y}_i)|, \quad (7)$$

$$\text{RMSE} = \sqrt{\frac{1}{N} \sum_{i=1}^N (y_i - \hat{y}_i)^2}, \quad (8)$$

$$\text{VAF} = \left[ 1 - \frac{\text{var}(y - \hat{y})}{\text{var}(y)} \right] \times 100, \quad (9)$$

where the measured and the predicted values are denoted by  $y$  and  $\hat{y}$ , respectively, and  $N$  is sample number. If values of parameters MAE and RMSE are closer to zero and the value of VAF is close to hundred, the model is considered as acceptable at the 95% confidence level.

To compare the goodness of fit of each RBFNN model, some representative hypotheses tests were conducted for the model construction process. Firstly, prior to performing a  $t$ -Student test, a Fisher's  $F$ -test was performed to test if the variances of two populations are equal [30]. After performing  $F$ -tests,  $p$ -values were obtained for each RBFNN model. If the  $p$ -values obtained are greater than 0.05, then the null hypothesis cannot be rejected [31]. In other words, there is no difference in variance of height measures between the two populations. Also, if the  $p$ -values  $> 0.05$ , a  $t$ -Student test can be performed for each RBFNN model by assuming the variances of two populations being equal. If the  $p$ -values  $< 0.05$ , a  $t$ -Student test can be performed for each RBFNN model by assuming the variances of two populations being unequal. A  $t$ -Student test was performed to test the null hypothesis that there is no difference between the means of two populations. After performing  $t$ -Student tests,  $p$ -values are obtained for each RBFNN model. If the  $p$ -values are above 0.05, the

mean of the predicted data is very close to the mean of experimental data.

## Results and discussion

The predicted activity concentration values of  $^{232}\text{Th}$ ,  $^{238}\text{U}$  and  $^{40}\text{K}$  using RBFNN-1, RBFNN-2, and RBFNN-3 models were compared with the determined activity concentration values of  $^{232}\text{Th}$ ,  $^{238}\text{U}$  and  $^{40}\text{K}$  from gamma spectrometry measurements for training and testing samples in Figs. 2, 3 and 4, respectively. Figures 2, 3 and 4 show that the predicted activity concentration values from each individual RBFNN model are found to be quite close to the determined activity concentration values for training and testing samples.

By taking into account this precise performance of each individual RBFNN model (Figs. 2, 3, 4), a generalized RBFNN model was developed for the prediction of activity concentration values of  $^{232}\text{Th}$ ,  $^{238}\text{U}$  and  $^{40}\text{K}$  in 126 geological materials. While developing the generalized RBFNN model, count rates in thorium, uranium, and potassium channels were selected as input parameters, and the activity concentration values of  $^{232}\text{Th}$ ,  $^{238}\text{U}$  and  $^{40}\text{K}$  were chosen as output parameters. The plots of the comparison of the predicted activity concentration values of  $^{232}\text{Th}$ ,  $^{238}\text{U}$  and  $^{40}\text{K}$  using the generalized model RBFNN with the determined activity concentration values of  $^{232}\text{Th}$ ,  $^{238}\text{U}$  and  $^{40}\text{K}$  from gamma spectrometry measurements are given in Figs. 5, 6 and 7, respectively, for training and testing sets. It can be noticed from Figs. 5, 6 and 7 that the generalized model RBFNN yields activity concentration values, which are very close to the determined activity concentration values from gamma spectrometry measurements.

The MAE, RMSE and VAF values represented by Eqs. (7), (8) and (9), respectively, were calculated to evaluate the performance of each individual and generalized RBFNN models developed in this study, which is given in Table 2 for each individual model and in Table 3 for the generalized model. It can be noticed from the computed performance parameters in Tables 2 and 3, all individual and generalized RBFNN models exhibit precise performance, which shows their usefulness and efficiency for determining activity concentration values of  $^{232}\text{Th}$ ,  $^{238}\text{U}$  and  $^{40}\text{K}$  in geological materials.

After performing Fisher's  $F$ -tests for individual RBFNN models,  $p$ -values were found as 0.498, 0.488 and 0.499 for the RBFNN-1, RBFNN-2 and RBFNN-3 models, respectively. From the generalized RBFNN model,  $p$ -values were found as 0.486, 0.492 and 0.499 for the prediction of activity concentration values of  $^{232}\text{Th}$ ,  $^{238}\text{U}$  and  $^{40}\text{K}$ , respectively. These  $p$ -values greater than 0.05 indicated that the null hypothesis cannot be rejected and so the variance of

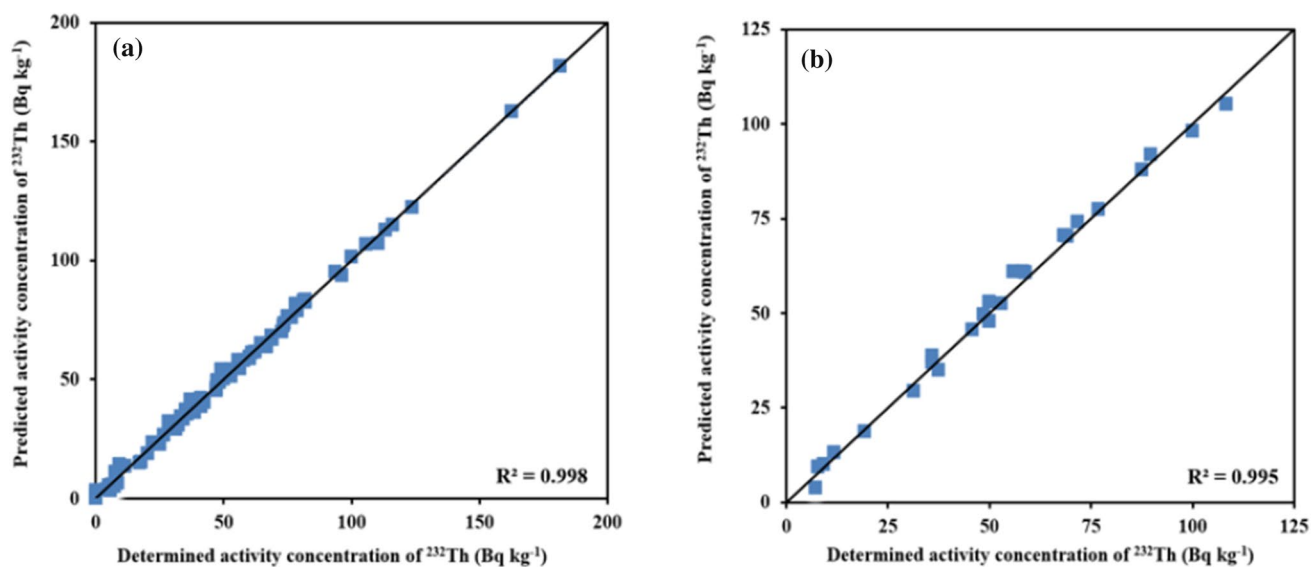


**Fig. 2** Comparison of determined activity concentration of  $^{232}\text{Th}$  with the predicted activity concentration of  $^{232}\text{Th}$  from RBFNN-1 model **a** for training set and **b** for testing set

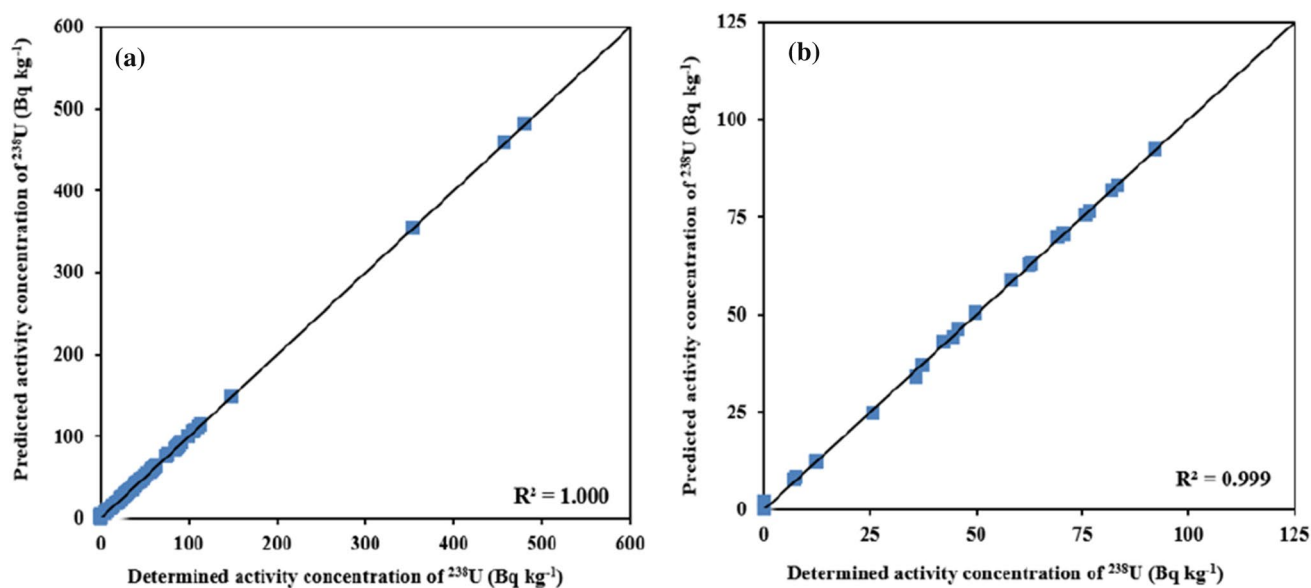


**Fig. 3** Comparison of determined activity concentration of  $^{238}\text{U}$  with the predicted activity concentration of  $^{238}\text{U}$  from RBFNN-2 model **a** for training set and **b** for testing set

determined and predicted activity concentration values are equal. Thus, a *t*-Student test was then performed for each individual RBFNN model and for the generalized model by assuming the variances of determined and predicted activity concentration values being equal. After performing *t*-Student tests, *p*-values were found as 0.969, 0.982 and 0.994 for the RBFNN-1, RBFNN-2 and RBFNN-3 models, respectively. From the generalized RBFNN model, *p*-values were found as 0.977, 0.984 and 0.994 for the prediction of activity

concentration values of  $^{232}\text{Th}$ ,  $^{238}\text{U}$  and  $^{40}\text{K}$ , respectively. These *p*-values are above 0.05, which indicated the mean of the predicted data is very close to the mean of experimental data. By considering *p*-values, it is suggested that individual and generalized RBFNN models are used for determining the activity concentrations of primordial radionuclides, namely,  $^{232}\text{Th}$ ,  $^{238}\text{U}$  and  $^{40}\text{K}$  of geological materials if count rates in thorium, uranium, and potassium channels are known.

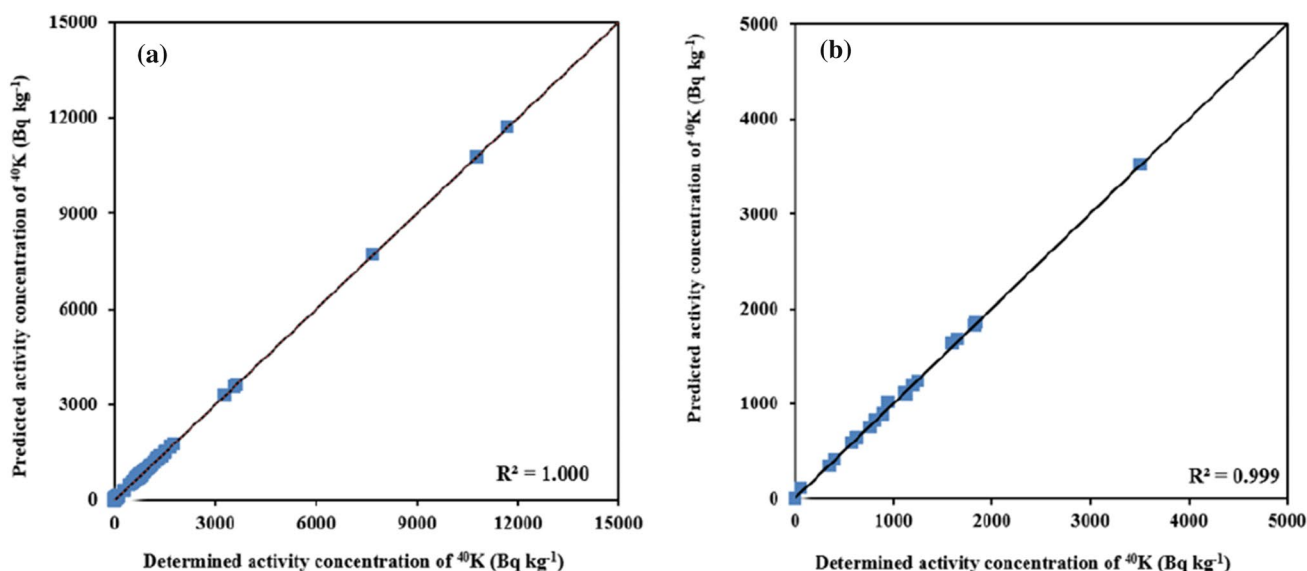


**Fig. 4** Comparison of determined activity concentration of  $^{40}\text{K}$  with the predicted activity concentration of  $^{40}\text{K}$  from RBFNN-3 model **a** for training set and **b** for testing set

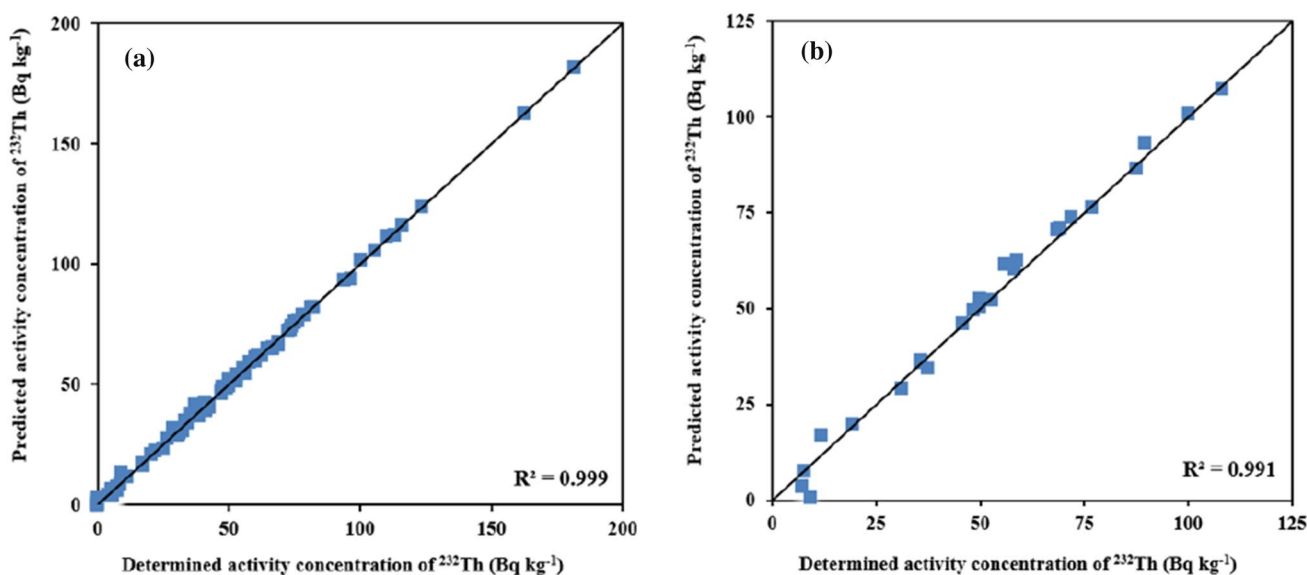


**Fig. 5** Comparison of determined activity concentration of  $^{232}\text{Th}$  with the predicted activity concentration of  $^{232}\text{Th}$  from the generalized RBFNN model **a** for training set and **b** for testing set

## Conclusions

In this study, three individual RBFNN models, namely, RBFNN-1, RBFNN-2 and RBFNN-3, were developed for the prediction of the activity concentrations of  $^{232}\text{Th}$ ,  $^{238}\text{U}$  and  $^{40}\text{K}$ , respectively. For this purpose, gamma spectrometry measurements of 126 different geological materials were used. The results obtained using each individual RBFNN model were compared with those determined

from the gamma spectrometry measurements. It is found that the values predicted from each RBFNN model match accurately with the experimental values. By considering the precise performance of each individual RBFNN model, a generalized RBFNN model was developed for predicting the activity concentrations of three radionuclides. The values predicted from the generalized RBFNN model are found to be very close to the experimental values. The study demonstrates that individual and generalized

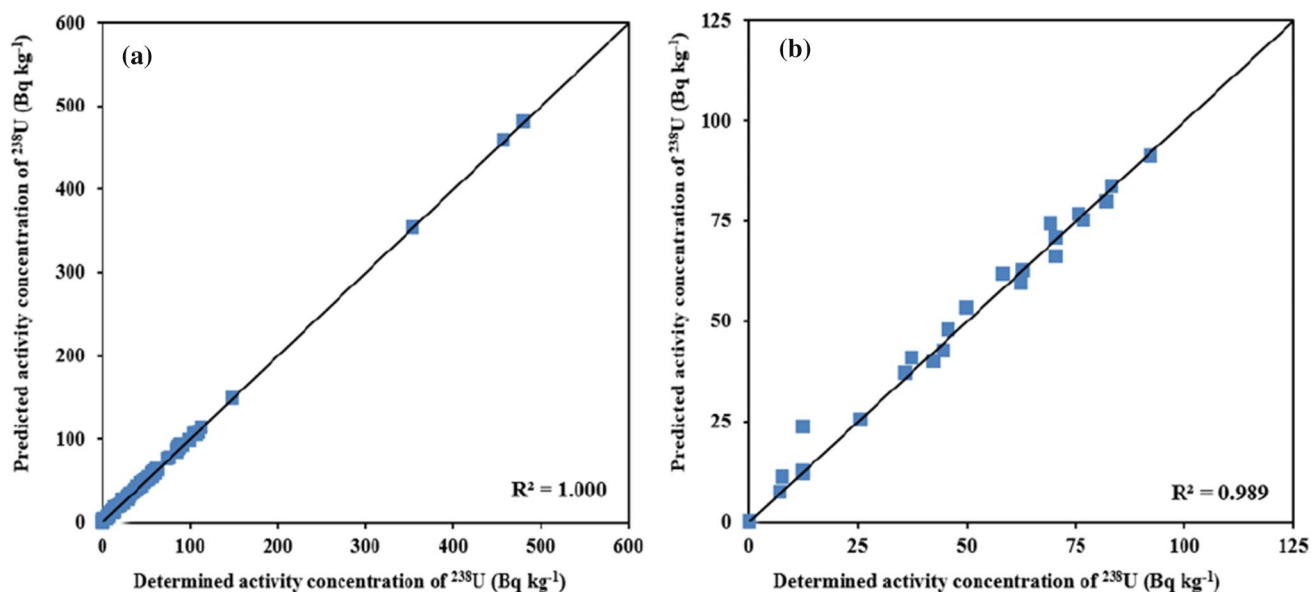


**Fig. 6** Comparison of determined activity concentration of  $^{238}\text{U}$  with the predicted activity concentration of  $^{238}\text{U}$  from the generalized RBFNN model **a** for training set and **b** for testing set

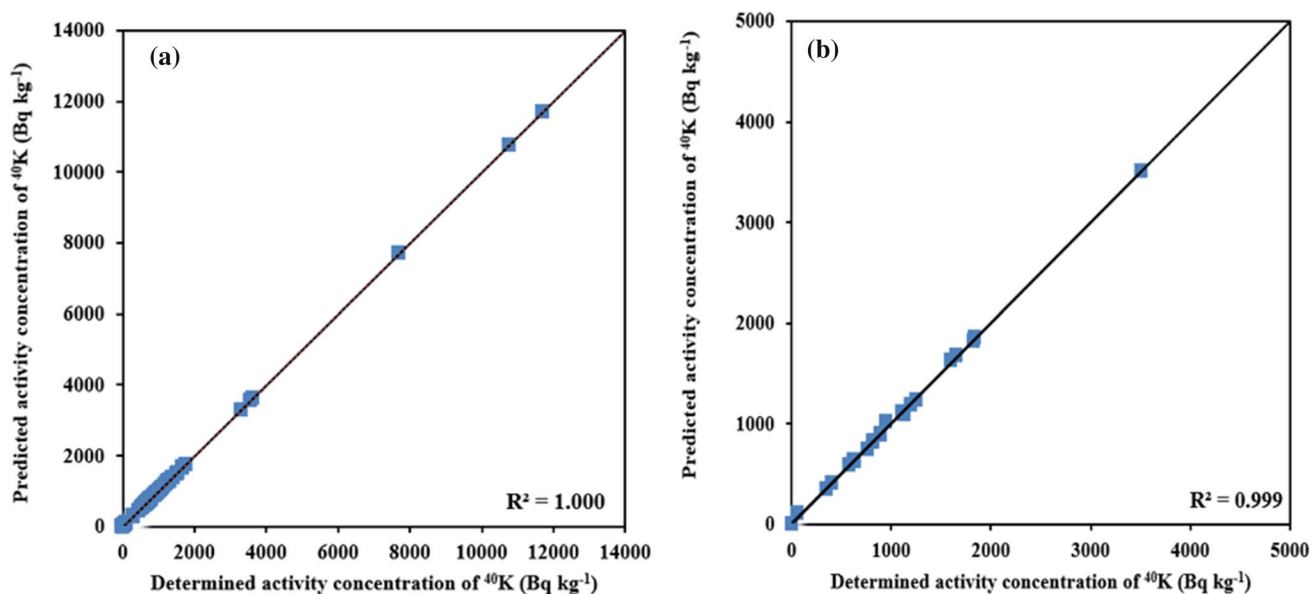


**Fig. 7** Comparison of determined activity concentration of  $^{40}\text{K}$  with the predicted activity concentration of  $^{40}\text{K}$  from the generalized RBFNN model **a** for training set and **b** for testing set

**Table 2** Performance indices ( $R^2$ , MAE, RMSE and VAF) of individual RBFNN models developed

Model	Data	$R^2$	MAE ( $\text{Bq kg}^{-1}$ )	RMSE ( $\text{Bq kg}^{-1}$ )	VAF (%)
RBFNN-1	Training set	0.998	1.34	1.75	99.78
	Testing set	0.995	1.85	2.16	95.51
RBFNN-2	Training set	0.999	0.59	0.92	99.99
	Testing set	0.999	0.51	0.72	99.94
RBFNN-3	Training set	1.000	3.46	6.30	99.99
	Testing set	0.999	12.64	21.58	99.91

**Table 3** Performance indices ( $R^2$ , MAE, RMSE and VAF) of the generalized RBFNN model developed

Radionuclide	Data	$R^2$	MAE (Bq kg <sup>-1</sup> )	RMSE (Bq kg <sup>-1</sup> )	VAF (%)
<sup>232</sup> Th	Training set	0.999	0.94	1.31	99.88
	Testing set	0.991	2.09	2.90	98.95
<sup>238</sup> U	Training set	1.000	0.89	1.22	99.97
	Testing set	0.989	2.11	3.17	98.81
<sup>40</sup> K	Training set	1.000	0.63	7.62	100.00
	Testing set	0.999	12.63	21.58	99.91

RBFNN models are quite efficient in predicting the activity concentrations of <sup>232</sup>Th, <sup>238</sup>U and <sup>40</sup>K of geological materials. Similar RBFNN models could be employed for different types of geological materials to predict the activity concentrations of <sup>232</sup>Th, <sup>238</sup>U and <sup>40</sup>K.

**Acknowledgements** The authors are grateful Dr. Zsolt Revay, Editor-in-Chief of Journal of Radioanalytical and Nuclear Chemistry, and two anonymous reviewers for their constructive criticism leading to extensive improvement in the revised manuscript.

## Declarations

**Conflict of interest** The authors declare that there is no conflict of interest regarding the publication of this paper.

## References

- UNSCEAR (2000) Sources and effects of ionizing radiation. United Nations, New York
- Hofstadter R (1949) The detection of gamma-rays with thallium-activated sodium iodide crystals. *Phys Rev* 75:796–810
- Pilakouta M, Pappa FK, Patiris DL, Tsabaris C, Kalfas CA (2018) A methodology for expanding the use of NaI(Tl) based spectrometry in environmental radioactivity measurements. *Appl Radiat Isot* 139:159–168
- Eker GBC, Çağlar İ (2019) A study on calculation of full energy peak efficiency of NaI(Tl) detectors using point source. *Cauc J Sci* 6(1):28–36
- Sahin L, Cavas M (2008) Natural radioactivity measurements in soil samples of Central Kutahya (Turkey). *Radiat Prot Dosim* 131:526–530
- Tabar E, Yakut H, Saç MM, Taşköprü C, İchedef M, Kuş A (2017) Natural radioactivity levels and related risk assessment in soil samples from Sakarya, Turkey. *J Radioanal Nucl Chem*. <https://doi.org/10.1007/s10967-017-5266-2>
- Shilpa GM, Anandaram BN, Mohankumari TL (2018) Measurement of activity concentration of primordial radionuclides in soil samples from Thirithahalli Taluk and the assessment of resulting radiation dose. *J Radioanal Nucl Chem* 316:501–511
- Al-Ghamdi A (2019) Health risk assessment of natural background radiation in the soil of Eastern Province, Saudi Arabia. *J Radiat Res Appl Sci* 12:219–225
- Bajoga A, Al-Dabbous A, Abdullahi A, Alazemi N, Bachama Y, Alaswad S (2019) Evaluation of elemental concentrations of uranium, thorium and potassium in top soils from Kuwait. *Nucl Eng Technol* 51(6):1636–2164
- Filgueiras RA, Silva AX, Ribeiro FCA, Lauria DC, Viglio EP (2019) Baseline, mapping and dose estimation of natural radioactivity in soils of the Brazilian state of Alagoas. *Radiat Phys Chem* 167:108332–108338
- Akbar A, Asley K, Şeref T, Fatemeh M (2020) Radiation hazards and natural radioactivity levels in surface soil samples from dwelling areas of North Cyprus. *J Radioanal Nucl Chem* 324:203–210
- Somsavath L, Giang TTP, Thang DD, Le N-T, Khong NK, Sounthone S, Hai-Nam T, Van LB (2020) Natural radioactivity measurement and radiological hazard evaluation in surface soils in a gold mining area and surrounding regions in Bolikhamxay Province, Laos. *J Radioanal Nucl Chem* 326:997–1007
- Srinivasa E, Rangaswamy DR, Suresh SN, Sannappa J (2022) Natural radioactivity levels and associated radiation hazards in soil samples of Chikkamagaluru District, Karnataka, India. *J Radioanal Nucl Chem* 331:1899–1906
- Roshani GH, Karami A, Salehizadeh A, Nazemi E (2017) The capability of radial basis function to forecast the volume fractions of the annular three-phase flow of gas–oil–water. *Appl Radiat Isot* 129:156–162
- Buhmann MD (2003) Radial basis functions: theory and implementations. Cambridge University Press, Cambridge
- Zadeh EE, Fegghi SAH, Roshani GH, Rezaei A (2016) Application of artificial neural network in precise prediction of cement elements percentages based on the neutron activation analysis. *Eur Phys J Plus* 131:167
- Alvar AA, Deevband MR, Ashtiyani M (2017) Neutron spectrum unfolding using radial basis function neural networks. *Appl Radiat Isot* 129:35–41
- Moody J, Darken CJ (1989) Fast learning in networks of locally-tuned processing units. *Neural Comput* 1(2):281–294
- Park J, Sandberg IW (1991) Universal approximation using radial basis-function networks”. *Neural Comput* 3(2):246–257
- Zayandehroodi H, Mohamed A, Shareef H, Mohammadjafari M (2010) Automated fault location in a power system with distributed generations using radial basis function neural networks. *J Appl Sci* 10:3032–3041
- Erzin S (2019) Application of artificial neural networks to gamma spectrometric measurements. PhD Thesis, Ege University, İzmir (Turkish with English abstract)
- Broomhead D, Lowe D (1988) Multivariable functional interpolation and adaptive networks. *Complex Syst* 2:321–355
- Ham F, Kostanic I (2001) Principles of neurocomputing for science and engineering. McGraw-Hill, New York
- Segal R, Kothari ML, Madhani S (2000) Radial basis function (RBF) network adaptive power system stabilizer. *IEEE Trans Power Syst* 15:722–727
- Szczurek A, Maciejewska M (2004) Recognition of benzene, toluene and xylene using TGS array integrated with linear and non-linear classifier. *Talanta* 64:609–617
- Haykin S (2009) Neural networks and learning machines, vol 3. Pearson, Upper Saddle River
- Yaprak G (1995) Matrix effects on gamma spectrometric analysis of radioactive materials and development a self absorption



- correction method. PhD Thesis, Ege University, İzmir (Turkish with English abstract)
28. Yaprak G, Aslani MAA (2010) External dose-rates for natural gamma emitters in soils from an agricultural land in West Anatolia. *J Radioanal Nucl Chem* 283:279–287
  29. Bors AG, Pitas I (1996) Median radial basis function neural network. *IEEE Trans Neural Netw* 7:1351–1364
  30. Snedecor GW, Cochran WG (1989) *Statistical methods*, 8th edn. Iowa State University Press, Ames
  31. Gupta AK (2010) Predictive modelling of turning operations using response surface methodology, artificial neural networks and support vector regression. *Int J Prod Res* 48:763–778

**Publisher's Note** Springer Nature remains neutral with regard to jurisdictional claims in published maps and institutional affiliations.